nextnano: General Purpose 3-D Simulations

Stefan Birner, Tobias Zibold, Till Andlauer, Tillmann Kubis, Matthias Sabathil, Alex Trellakis, and Peter Vogl

(Invited Paper)

***Abstract*—nextnano is a semiconductor nanodevice simulation tool that has been developed for predicting and understanding a wide range of electronic and optical properties of semiconductor nanostructures. The underlying idea is to provide a robust and generic framework for modeling device applications in the field of nanosized semiconductor heterostructures. The simulator deals with realistic geometries and almost any relevant combination of materials in one, two, and three spatial dimensions. It focuses on an accurate and reliable treatment of quantum mechanical effects and provides a self-consistent solution of the Schrödinger, Poisson, and current equations. Exchange-correlation effects are taken into account in terms of the local density scheme. The electronic structure is represented within the single-band or multiband $\mathbf{k} \cdot \mathbf{p}$ envelope function approximation, including strain. The code is not intended to be a "black box" tool. It requires a good understanding of quantum mechanics. The input language provides a number of tools that simplify setting up device geometry or running repetitive tasks. In this paper, we present a brief overview of nextnano and present four examples that demonstrate the wide range of possible applications for this software in the fields of solid-state quantum computation, nanoelectronics, and optoelectronics, namely, 1) a realization of a qubit based on coupled quantum wires in a magnetic field, 2) and 3) carrier transport in two different nano-MOSFET devices, and 4) a quantum cascade laser.**

***Index Terms*—Carrier transport, electronic structure, magnetic field, quantum, quantum wire, simulation, technology computer-aided design (TCAD).**

I. Overview of next**nano**

A VERSATILE software package, next**nano**, is used for the simulation of nanometer-scale semiconductor quantum structures and devices, providing insight into a wide range of physical properties [1]. next**nano** focuses on nanostructures where quantum mechanical effects such as electronic band structures, optical matrix elements, magnetic field effects, or tunneling effects play a vital role. Using an extensive materials database for Si/Ge, II–VI, and III–V materials, including nitride semiconductors, their binary, ternary, and quaternary alloys, and both zincblende and wurtzite crystal structures, a wide variety of quantum structures with realistic composite device geometries can be modeled.

The input required by the software is specified by a text file that defines the geometry, the materials of the nanostructure, and all other information needed to describe the physical system under consideration. The program flow is organized as follows. Since most nanostructures consist of strained materials, next**nano** starts by performing a global strain minimization based on a macroscopic elasticity theory. Once the strain field has been calculated, the piezoelectric and the pyroelectric charges are determined (the latter are relevant for wurtzite structure materials). Consequently, the electronic structure is calculated within a single-band or multiband $\mathbf{k} \cdot \mathbf{p}$ envelope function approximation. Subsequently, the Poisson equation, current equation, and Schrödinger equations are solved self-consistently with respect to one another. Finally, in a postprocessing step, the optical interband and the intraband transition matrix elements between wave functions and excitonic properties in confined systems can be calculated. We have extended next**nano** to include semiconductor–electrolyte interactions self-consistently in order to be able to investigate ion-sensitive field-effect transistors (ISFETs) or silicon nanowire-based biosensors for DNA detection (i.e., 2- and 3-D electrolyte simulation). Another topic of our ongoing research activities is the modeling of gas sensors. The gas molecules adsorb at the semiconductor surface and lead to a surface charge density that controls the current in such devices. This effect resembles the variation of the interface charge density in ISFET devices. Finally, spintronic devices and solid-state-based quantum information systems are the most recent applications that require novel features to be implemented into our software.

In order to simulate nanodevice properties under an applied bias, next**nano** includes three models for the carrier transport for 1-, 2-, and 3-D simulations. One is a Wentzel–Kramer–Brillouin (WKB)-type approach that we termed the quantum-drift-diffusion (QDD) method. In this approach, we assume that the carriers are locally in equilibrium and can be characterized by a local Fermi level. A second approach, which is termed the contact block reduction (CBR) method [2], [3], is based on an efficient method to compute the ballistic current through an arbitrarily shaped open system with any number of leads. Recently, we implemented a third quantum transport approach that is based on a fully self-consistent version of the nonequilibrium Green's function (NEGF) technique [4],

Manuscript received February 5, 2007; revised May 23, 2007. This work was supported in part by the Deutsche Forschungsgemeinschaft (SFB 631), by the Österreichische FWF (Projekt IR-ON F025), and by the German Excellence Initiative via the Nanosystems Initiative Munich (NIM). The review of this paper was arranged by Editor E. Sangiorgi.

S. Birner, T. Zibold, T. Andlauer, T. Kubis, and A. Trellakis are with the Walter Schottky Institute, Technical University of Munich, 85748 Garching, Germany (e-mail: stefan.birner@nextnano.de).

M. Sabathil was with the Walter Schottky Institute and the Physics Department of the Technical University of Munich, 85748 Garching, Germany. He is now with OSRAM Opto Semiconductors, 93055 Regensburg, Germany.

P. Vogl is with the Theoretical Semiconductor Physics Group, Walter Schottky Institute and the Department of Physics, Technical University of Munich, 85748 Garching, Germany (e-mail: vogl@wsi.tum.de).

Color versions of one or more of the figures in this paper are available online at http://ieeexplore.ieee.org.

Digital Object Identifier 10.1109/TED.2007.902871

0018-9383/$25.00 © 2007 IEEE

and we will discuss some of its results here. It includes the retarded and the lesser Green's functions, as well as all relevant scattering processes, in a self-consistent manner. Since this approach is extremely computation-intensive, it is currently limited to effectively 1-D simulations such as resonant tunneling or quantum cascade laser (QCL) structures. Finally, we are currently working on a module that combines 2-D Monte Carlo simulations [5] and a $\mathbf{k} \cdot \mathbf{p}$-based electronic structure for uniaxially stressed pMOSFETs [6], [7].

The maintenance of the original next**nano** Fortran 90 code (termed next**nano**^{3}) became increasingly difficult due to its roughly 250 000 lines of code. For this reason, a completely new version has been developed during the last three years. It is termed next**nano**++ and is coded in a modular and strictly object-oriented fashion in C++. Only the very core algebraic libraries are still based on Fortran.

This paper supplements two previously published articles about next**nano** [8], [9]. Here, we will present several applications that highlight the capabilities of our simulation software. In particular, we discuss several carrier transport issues, present a quantum wire-based qubit realization, where a magnetic field is used for efficient wave function engineering, and present some NEGF results. We refer to [8] for a discussion of the code structure, a summary of the implemented numerical methods, and a comparison with related software tools.

II. Qubit Manipulation

An important but sometimes ignored aspect of the numerical solution of the Schrödinger equation in a magnetic field is gauge invariance. Since the vector potential increases linearly as a function of position, its values tend to be one or two orders of magnitude larger at the boundaries of the simulation region than at the center. Therefore, the numerical solutions depend sensitively on the chosen gauge for nonzero magnetic field, even if the zero field wave functions are small at the boundaries. This problem was successfully addressed in [10] for single-band nonrelativistic Hamiltonians. We have recently generalized this scheme for arbitrary envelope function Hamiltonians in a way that ensures manifestly gauge invariant results for any magnetic field [8], [9].

Here, we apply this method to coupled quantum wires in a longitudinal magnetic field. Two GaAs quantum wells, each with a width of 14.5 nm, are vertically stacked along the y-direction and are separated by a thin $Al_{0.32}Ga_{0.68}As$ tunnel barrier that is 1 nm wide. Electrons are provided by two delta-doped layers on each side of the double quantum well structure $(\delta_{\text{top}} = 2.1 \times 10^{12}\ \text{cm}^{-2}, \delta_{\text{bottom}} = 2.9 \times 10^{11}\ \text{cm}^{-2})$. The upper well is 60 nm below the surface, where we pin the Fermi energy by surface states in the middle of the band gap. A top-gate voltage of 0.04 V is applied to this Schottky contact that leads to nearly symmetric quantum wells. The top-gate voltage can be used to tune the electron density, i.e., to shift the ground state from the top to the bottom wells (the first excited state is then located in the opposite well) or to vary the degree of wave function mixing (bonding/antibonding) between the two wells. The actual quantum wires are obtained by wet-etching nanogrooves into the semiconductor surface,

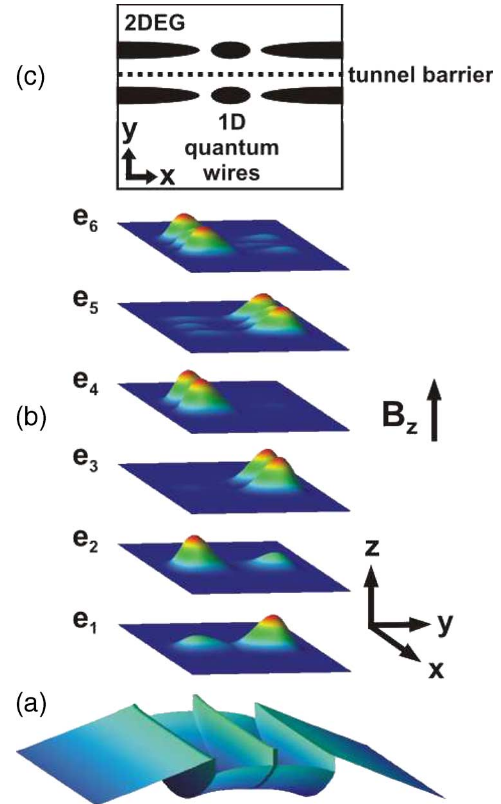

Fig. 1. (a) Two-dimensional conduction band profile $E_c(x, y)$ of the coupled quantum wires in the (x, y) plane, with $z =$ const. (b) Square of the wave functions $|\psi_i(x, y)|^2$ for the six lowest electron eigenstates at a magnetic field of 4.5 T oriented along the wire (z)-direction. (c) Schematic cross section of the electron systems (dark). The 1-D quantum wires are formed by electrostatically depleting the 2DEG.

which locally deplete the 2-D electron gas (2DEG) of the GaAs/AlGaAs double quantum well heterostructure and produce two electrostatically defined quantum wires on top of each other [Fig. 1(c)]. The experimental details are described in [11]. Such wires are short ballistic 1-D electron systems and recently attracted attention because controllable coupling can be achieved, making such devices interesting for solid-state quantum information processing. Superposition states are formed by tunnel coupling between the quantum wires. They can be altered by an applied magnetic field along the wire direction leading to tunable wave function mixing, in addition to the mixing produced by the top gate. To implement such quantum logic devices in quantum circuits, one would like to understand and have detailed control over all involved electron levels, which calls for a realistic modeling such as provided by next**nano**. We have solved the 2-D Schrödinger–Poisson equation of the double quantum well heterostructure for electrons self-consistently, taking into account the spatially varying material parameters. We have modeled the confinement due to the nanogrooves by a parabolic potential along the x-direction and set its characteristic energy such that it matches the observed low-lying level spacing of 10 meV. For the resulting 2-D confinement potential [Fig. 1(a)], we have calculated the electronic eigenstates as a function of a magnetic field oriented along the wire (z)-direction, i.e., perpendicular to the 2-D confinement potential landscape. For the conduction band

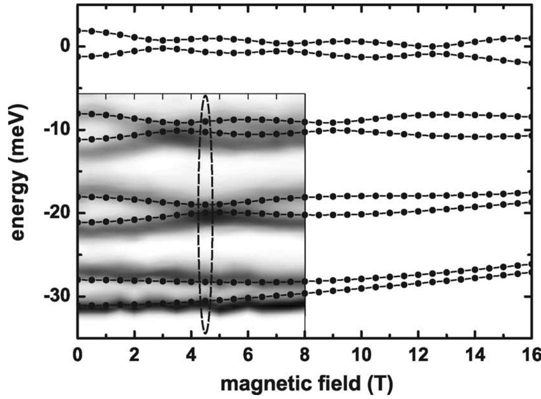

Fig. 2. Calculated energy spectrum of the eight lowest electron eigenstates of the coupled quantum wires as a function of magnetic field strength (the lines are a guide to the eye). The dashed ellipse highlights the six eigenstates at 4.5 T, which are plotted in Fig. 1(b). For comparison, the rectangle shows the gray-scale plot of the transconductance maxima versus the top gate voltage and magnetic field from 0 to 8 T (experimental data after [11, Fig. 8(b)]). Note that the top gate voltage was scaled so that the subband energies approximately align with the energy scale.

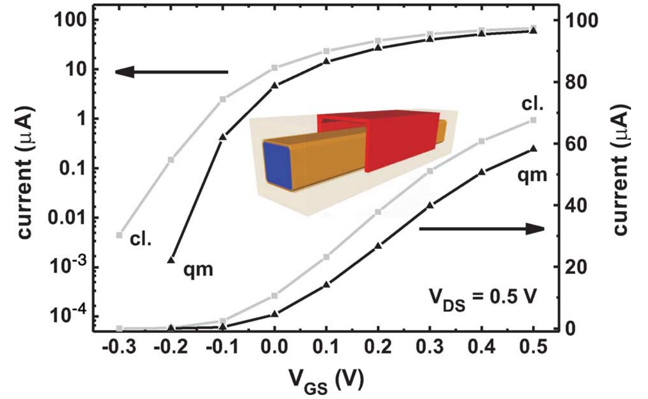

Fig. 3. Current–voltage characteristics of a triple-gate Si MOSFET with a 5 × 5-nm channel and 25-nm gate length (inset). The graph shows the I–V curves for classical (gray line) and quantum mechanical (black line) simulations, respectively. In the latter case, the current is smaller.

offset between GaAs and $Al_{0.32}Ga_{0.68}As$, we have used a value of 0.30 eV.

Our numerical calculations of the energy spectrum (Fig. 2) reproduce the experimental transconductance maxima (cf., [11, Fig. 8(b)]) very well. These maxima directly image the subband edges of 1-D ballistic electron transport in electron waveguides. One can clearly see the occurrence of level anticrossings at certain magnetic fields. For those energies, the tunneling coupling is significantly reduced or vanishes. This is the case, for example, for the third and fourth eigenstates in Fig. 2 for a magnetic field strength of 4.5 T. Consequently, the probability amplitudes of these states [labeled e_3 and e_4 in Fig. 1(b)] are not smeared out any longer over the two wires, in contrast to the other states, which still show wave function tunneling. Such a structure can be considered a qubit with logic states that are represented by the presence of the electron in the upper or lower quantum wire, respectively, and a coupling window that allows for electron transfer between these wires. By varying the magnetic field, one is able to switch between the different logic states. Note that the energy spectrum, which is shown in Fig. 2, does not include the (very small) spin splitting. Our results agree nicely qualitatively with analytic studies [12] that ignored charge redistribution due to doping and applied gate voltages. An important difference is the fact that we find an anticrossing behavior, whereas the analytical results always yield a crossing behavior, which is equivalent to assuming that the tunnel splitting vanishes completely for some fields. The challenge in this concept is to grow symmetric quantum wire structures in order to reduce the tunnel splitting as much as possible.

III. Carrier Transport

Modeling carrier transport in nanostructures poses quite a challenge if one wishes to treat scattering and quantum interference effects on an equal footing. Although this challenge can be met using NEGF techniques [13], [14], these methods require immense computational resources for any but (quasi) 1-D simulations. For this reason, next**nano** includes two simpler transport models for studying the electronic structure and carrier transport under an applied bias in 2- or 3-D devices, namely, the QDD method [15], [16] and the CBR method [2], [3]. The latter is based on the solution of the Schrödinger equation for an open ballistic quantum mechanical system and does not include any inelastic scattering mechanisms or decoherence effects.

The QDD method is a WKB-based approach. It invokes the current–density relation that originates in the first moment of the Boltzmann equation but uses quantum mechanics to calculate the carrier density. In many nanostructures, the current is limited by several heterobarriers and, therefore, very small. In such a situation, it is reasonable to assume that the carriers are close to a local thermodynamic equilibrium and obey a Fermi–Dirac statistics with a position-dependent quasi-Fermi level. This position dependence can, in principle, lead to the unphysical result that quantum states get occupied nonuniformly in space. Whenever the potential varies slowly in space, however, and the total current through the device is small, such a situation does not occur, as we have carefully assessed by many test cases. These current equations have to be solved self-consistently with the Poisson equation in order to determine the current, the carrier density, and the potential. In addition, an empirical mobility model has to be employed. To illustrate this method, we have calculated the I–V curve of a triple-gate MOSFET for a source–drain voltage of $V_{\mathrm{DS}} = 0.5$ V (Fig. 3). The Si wire forming the channel is the same as in [17] and has a 5 × 5-nm cross section. The total length of the Si wire is 45 nm, the gate length is 25 nm, and the oxide thickness is 1.5 nm. The quantum mechanically calculated electron density in the open channel for $V_{\mathrm{GS}} = 0.5$ V and $V_{\mathrm{DS}} = 0$ V has been shown in a preceding paper [8]. With next**nano++**, the fully coupled system of 3-D Poisson, 3-D Schrödinger, and 3-D current equations can be solved so efficiently that we are now able to present the entire current–voltage characteristics. With next**nano++**, a single point of the I–V curve requires less than 2-h computer time for $115 \times 21 \times 21 = 50\,715$ grid points. Although this is two orders of magnitude slower than the classical drift-diffusion calculation, it is more than one order of magnitude faster than the old version of next**nano**. We

would like to mention that we found solving all three types of equations simultaneously to be much more efficient, rather than solving first the coupled Schrödinger–Poisson equation, subsequently the current equation, and iterating those two sets in an outer loop. Our new procedure reduces the number of times that the eigenvalues have to be calculated. Finally, we note that for silicon, three separate Schrödinger equations have to be solved due to the anisotropic effective mass tensor of silicon.

We now turn to ballistic current calculations that are based on the CBR method. This method is suitable for extremely small devices or very low temperatures, where the elastic and inelastic scattering lengths exceed the geometrical device size. This situation occurs, for instance, in quantum interference devices [18] and within (but not in front of) resonant tunneling structures. For these systems, we have employed the Landauer–Büttiker formalism [19], [20] to calculate the ballistic current $J_{\lambda\lambda'}$ between all contacts λ and λ' [21]. This formula generally involves an integration over all quantum numbers that characterize the lead states. To simplify the equations, we suppress their momentum dependence (which is, however, included in the calculation) and write the ballistic current in the form

$$J_{\lambda\lambda'} = \frac{e}{\pi\hbar} \int dE T_{\lambda\lambda'}(E) \left[f_\lambda(E) - f_{\lambda'}(E)\right] \tag{1}$$

where E is the energy, $f_\lambda(E)$ is the equilibrium distribution function inside contact λ, and $T_{\lambda\lambda'}(E)$ is the transmission function between contacts λ and λ'. These transmission functions are calculated using the retarded single particle Green's function [4]. Since the transport is assumed to be ballistic both inside the device and within the contact regions, scattering only occurs at the contact-device boundaries, and the self-energy matrices vanish everywhere else. This allows us to use the CBR method [2] to determine $T_{\lambda\lambda'}$ efficiently. We are currently investigating an extension of this method that includes scattering within a Büttiker probe model [20].

The CBR method, in its original form, did not include charge self-consistency. However, charge self-consistency cannot be neglected for nano-MOSFET simulations and actually plays a vital role for those devices. We have therefore generalized this method to include charge self-consistency. Whereas a mere calculation of the transmission function requires the calculation of the retarded Green's function matrix elements only between contact points, the carrier density also requires matrix elements between the contacts and the interior of the device. Fortunately and importantly, no interior–interior matrix elements need to be calculated in the ballistic case, so that the basic ideas of the CBR method still apply, even when charge self-consistency is taken into account. For the details that are far beyond the scope of this paper, see [22].

Here, we apply the self-consistent variant of the CBR method to a double-gate MOSFET. The geometry and doping profile of this MOSFET have been taken in [23]. The band structure is modeled by a single parabolic band with anisotropic effective masses for silicon and a spherical mass for the oxide. The gate leakage due to tunneling through the oxide barriers is fully included in this model. A very interesting and somewhat unexpected result of our calculations is the significance of exchange and correlation (XC) effects for MOSFET devices, particularly near the ON/OFF threshold voltage. High doping concentrations in a double-gate MOSFET structure near the contacts lead to a spatially highly inhomogeneous carrier density, which leads to strong electron–electron interaction effects. next**nano** takes these effects into account within the local density functional theory (DFT, LDA). The XC potentials depend only on the local density and can be evaluated easily within the global self-consistency cycle [22]. Concretely, the inclusion of XC increases the barrier height along the channel for an applied source–drain voltage of 0.05 V and zero gate voltage by roughly 10 meV. This can be explained by the fact that the dominant exchange potential is always attractive and proportional to some power of the electron density. It amounts to approximately −70 meV in the highly doped regions. The key point is that its magnitude is much lower in the intrinsic region of the channel. This automatically leads to an effective increase in the total potential and leads to the formation of an effective barrier in the intrinsic part of the channel. The shape of the effective potential across the channel resembles that of a classical solution and suppresses the density in the channel, compared to a Hartree calculation that ignores these XC effects. This effect can be most clearly seen in the transfer characteristics of the device, as illustrated in Fig. 4, where the source–drain current is plotted as a function of the gate voltage for the Hartree solution (solid line) and for the calculation that includes the XC effects (dashed line). Another important consequence of the electron–electron interaction is the gate leakage current (not shown in the figure) which, in the OFF-region of the device below −0.2 V, turns out to be roughly one order of magnitude higher than without XC effects. Thus, inhomogeneous doping profiles in nano-MOSFETS have the drawback of increasing the residual current in the OFF-state of the device, and this is an unavoidable consequence of the electron–electron interaction.

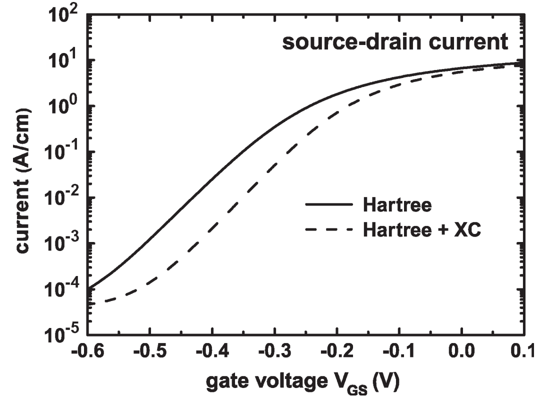

Fig. 4. Transfer characteristics of the ballistic double-gate MOSFET comparing the results of the pure Hartree calculation (solid line) with the results from the exchange-correlation calculation (dashed line).

Recently, we have performed a detailed assessment of the QDD method by comparing it with fully quantum mechanical and self-consistent NEGF calculations [8], [14]. For small biases, we found that the NEGF results agree excellently with the QDD method even though the balance between the carrier concentration outside and inside the quantum well is not

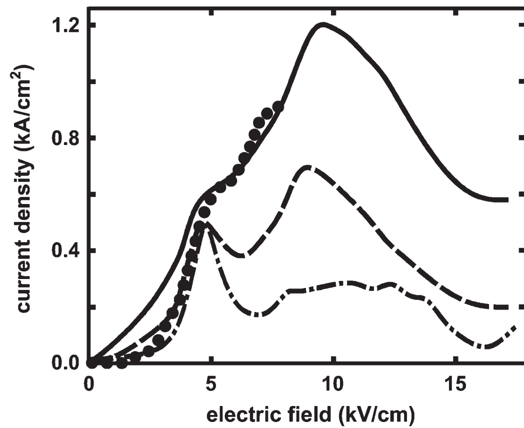

Fig. 5. I–V curve of the active region of the GaAs/AlGaAs QCL of [26] at 100 K. The fully self-consistent NEGF calculation (black solid line) agrees well with the experiment (dots), in contrast to the results with perfectly smooth interfaces (dashed line). Ballistic calculations (dash–dotted line) grossly underestimate the current density for all fields.

trivial to achieve. The NEGF method is extremely powerful for unipolar devices such as quantum well infrared photodetectors, resonant tunneling diodes, and QCLs, as it allows one to gain a predictive insight into their physical processes, namely, inelastic scattering, tunneling, population inversion, and optical gain. In our implementation of the NEGF method, acoustic phonon, polar–optical phonon, impurity, and interface roughness scattering are incorporated within the self-consistent Born approximation, maintaining the nonlocality of the self-energies. In addition, nonparabolicity effects are accounted for by energy-dependent effective masses. Detailed results for the carrier transport and optical gain in a terahertz QCL structure, where multiple scattering, interference effects, carrier confinement, and capture play an equally important role, will be presented in a separate paper [24]. The previously neglected [25] momentum and energy dependence of the scattering mechanisms is shown to have a significant influence on all QCL device characteristics. The electron–electron scattering is incorporated self-consistently within the Hartree approximation. The coupling between the lesser and the retarded Green's function is fully taken into account. This way, all scattering states, transition probabilities, and occupancies are calculated self-consistently with one another. This avoids artifacts such as the violation of Pauli blocking, which has plagued previous schemes.

Fig. 5 shows the calculated current–voltage characteristics of the active region for the GaAs/AlGaAs quantum cascade structure of [26]. The black solid line results from the full NEGF calculation, with all mentioned scattering mechanisms included. For a field of approximately 4 kV/cm, all relevant electronic states in the active region are energetically aligned, which leads to the corresponding peak in the current density. Importantly, the incoherent scattering through rough interfaces broadens the linewidths of the electronic states significantly. This effect reduces the peak-to-valley ratio, as compared to the situation with smooth interfaces (dashed line), and markedly increases the current that is no longer limited by strict lateral momentum conservation. The main peak in the current density at 9.3 kV/cm results from a combined longitudinal-optic-phonon emission and tunneling process from the lower laser level. Since quantum cascade structures are basically resonant tunneling diodes, they may seem suitable for modeling with ballistic current models. Fig. 5 shows, however, that a ballistic calculation (dash–dotted line) underestimates the current in a QCL structure fairly dramatically.

IV. Summary

In this paper, we have presented some recent applications of the next**nano** software. We have presented calculations of the energy spectrum of coupled quantum wires in a magnetic field and demonstrated how next**nano** can help in wave function engineering and the design of qubits. For a 2-D double-gate MOSFET, we have shown that the exchange-correlation potential has a significant influence on the device characteristics of nanoscale transistors. For a 3-D triple-gate MOSFET, we have calculated the current with a QDD model and compared it to the result obtained with a classical drift-diffusion model. Finally, we showed that the sophisticated I–V characteristics of QCL structures can be well reproduced by our recently developed NEGF transport model.

Acknowledgment

The authors would like to thank S. Selberherr, H. Kosina, and F. Stern for the helpful comments and encouragement in the early stages of the development of the next**nano** software. S. Birner would like to thank M. Povolotskyi for helpful discussions.

References

[1] See next**nano** Web site for executables and documentation. [Online]. Available: http://www.wsi.tum.de/nextnano3
[2] D. Mamaluy, M. Sabathil, and P. Vogl, "Efficient method for the calculation of ballistic quantum transport," *J. Appl. Phys.*, vol. 93, no. 8, pp. 4628–4633, Apr. 2003.
[3] D. Mamaluy, D. Vasileska, M. Sabathil, T. Zibold, and P. Vogl, "Contact block reduction method for ballistic transport and carrier densities of open nanostructures," *Phys. Rev. B, Condens. Matter*, vol. 71, no. 24, pp. 245 321-1–245 321-14, 2005.
[4] S. Datta, *Electronic Transport in Mesoscopic Systems*. Cambridge, U.K.: Cambridge Univ. Press, 1997.
[5] R. Oberhuber, G. Zandler, and P. Vogl, "Subband structure and mobility of two-dimensional holes in strained Si/SiGe MOSFET's," *Phys. Rev. B, Condens. Matter*, vol. 58, no. 15, pp. 9941–9948, Oct. 1998.
[6] E. Wang, P. Matagne, L. Shifren, B. Obradovic, R. Kotlyar, S. Cea, J. He, Z. Ma, R. Nagisetty, S. Tyagi, M. Stettler, and M. D. Giles, "Quantum mechanical calculation of hole mobility in silicon inversion layers under arbitrary stress," in *IEDM Tech. Dig.*, 2004, pp. 147–150.
[7] X.-F. Fan, L. F. Register, B. Winstead, M. C. Foisy, W. Chen, X. Zheng, B. Gosh, and S. K. Banerjee, "Hole mobility and thermal velocity enhancement for uniaxial stress in Si up to 4 GPa," *IEEE Trans. Electron Devices*, vol. 54, no. 2, pp. 291–296, Feb. 2007.
[8] A. Trellakis, T. Zibold, T. Andlauer, S. Birner, R. K. Smith, R. Morschl, and P. Vogl, "The 3D nanometer device project *nextnano*: Concepts, methods, results," *J. Comput. Electron.*, vol. 5, no. 4, pp. 285–289, 2006.
[9] S. Birner, S. Hackenbuchner, M. Sabathil, G. Zandler, J. A. Majewski, T. Andlauer, T. Zibold, R. Morschl, A. Trellakis, and P. Vogl, "Modeling of semiconductor nanostructures with next**nano**^{3}," *Acta Phys. Pol. A*, vol. 110, no. 2, pp. 111–124, 2006.
[10] M. Governale and C. Ungarelli, "Gauge-invariant grid discretization of the Schrödinger equation," *Phys. Rev. B, Condens. Matter*, vol. 58, no. 12, pp. 7816–7821, Sep. 1998.
[11] S. F. Fischer, G. Apetrii, U. Kunze, D. Schuh, and G. Abstreiter, "Tunnel-coupled one-dimensional electron systems with large subband separations," *Phys. Rev. B, Condens. Matter*, vol. 74, no. 11, pp. 115 324-1–115 324-7, Sep. 2006.

[12] L. G. Mourokh, A. Y. Smirnov, and S. F. Fischer, "Vertically coupled quantum wires in a longitudinal magnetic field," *Appl. Phys. Lett.*, vol. 90, no. 13, pp. 132 108-1–132 108-3, Mar. 2007.

[13] R. Lake, G. Klimeck, R. C. Bowen, and D. Jovanovic, "Single and multiband modeling of quantum electron transport through layered semiconductor devices," *J. Appl. Phys.*, vol. 81, no. 12, pp. 7845–7869, Jun. 1997.

[14] T. Kubis and P. Vogl, "Self-consistent quantum transport theory: Applications and assessment of approximate models," *J. Comput. Electron.*, vol. 6, no. 1–3, pp. 183–186, 2007.

[15] S. Hackenbuchner, "Elektronische Struktur von Halbleiter-Nanobauelementen im thermodynamischen Nichtgleichgewicht," in *Selected Topics of Semiconductor Physics and Technology*, vol. 48, G. Abstreiter, M.-C. Amann, M. Stutzmann, and P. Vogl, Eds. Walter Schottky Inst., TU Munich, 2002.

[16] M. Sabathil, S. Hackenbuchner, J. A. Majewski, G. Zandler, and P. Vogl, "Towards fully quantum mechanical 3D device simulations," *J. Comput. Electron.*, vol. 1, no. 1/2, pp. 81–85, 2002.

[17] G. Fiori and G. Iannaccone, "Simulation of one dimensional subband transport in ultra-short silicon nanowire transistors," in *Proc. 6th Eur. Conf. ULIS*, Bologna, Italy, 2005, pp. 163–166.

[18] M. Sabathil, D. Mamaluy, and P. Vogl, "Prediction of a realistic quantum logic gate using the contact block reduction method," *Semicond. Sci. Technol.*, vol. 19, no. 4, pp. S137–S138, Apr. 2004.

[19] R. Landauer, "Conductance from transmission: Common sense points," *Phys. Scr.*, vol. T42, pp. 110–114, 1992.

[20] M. Büttiker, "Symmetry of electrical conduction," *IBM J. Res. Develop.*, vol. 32, no. 3, pp. 317–334, May 1988.

[21] A. Di Carlo, P. Vogl, and W. Pötz, "Theory of Zener tunneling and Wannier–Stark states in semiconductors," *Phys. Rev. B, Condens. Matter*, vol. 50, no. 12, pp. 8358–8377, Sep. 1994.

[22] M. Sabathil, "Opto-electronic and quantum transport properties of semiconductor nanostructures," in *Selected Topics of Semiconductor Physics and Technology*, vol. 67, G. Abstreiter, M.-C. Amann, M. Stutzmann, and P. Vogl, Eds. Walter Schottky Inst., TU Munich, 2005.

[23] S. Hasan, J. Wang, and M. Lundstrom, "Device design and manufacturing issues for 10 nm-scale MOSFETs: A computational study," *Solid State Electron.*, vol. 48, no. 6, pp. 867–875, Jun. 2004.

[24] T. Kubis, C. Yeh, and P. Vogl, "Quantum theory of transport and optical gain in quantum cascade lasers," *Phys. Stat. Sol. C.* submitted for publication.

[25] A. Wacker, "Semiconductor superlattices: A model system for nonlinear transport," *Phys. Rep.*, vol. 357, no. 1, pp. 1–111, Jan. 2002.

[26] H. Callebaut, S. Kumar, B. S. Williams, Q. Hu, and J. L. Reno, "Analysis of transport properties of terahertz quantum cascade lasers," *Appl. Phys. Lett.*, vol. 83, no. 2, pp. 207–209, Jul. 2003.

Stefan Birner was born in Hirschau, Germany, in 1975. He received the Vordiplom degree in physics from the University of Bayreuth, Bayreuth, Germany, and the Master of Physics (MPhys) degree from the University of Exeter, Exeter, U.K., in 2000. He is currently working toward the Ph.D. degree in physics in the Walter Schottky Institute, Technical University of Munich, Garching, Germany.

In 2000, he was with the Physics Department, The Ohio State University, Columbus, where he performed molecular dynamics studies of defects in silicon.

Mr. Birner is a member of the Student MemberChip Program of Infineon Technologies and is Founder of next**nano**^{3}, which is a spin-off from the Walter Schottky Institute, which provides support to the next**nano**^{3} software.

Tobias Zibold was born in Bietigheim-Bissingen, Germany, in 1977. He received the Diplom degree in physics from the University of Tübingen, Tübingen, Germany. He is currently working toward the Ph.D. degree in physics in the Walter Schottky Institute, Technical University of Munich, Garching, Germany.

From 2000 to 2001, he was with the Physics Department, University of Massachusetts, Amherst. His current research interests are ballistic quantum transport and semiconductor-based quantum logic gates.

Mr. Zibold is a member of the Qimonda Academic Partnership Program.

Till Andlauer was born in Herne, Germany, in 1979. He received the Diplom degree in physics from the Technical University of Munich, Garching, Germany, in 2005. He is currently working toward the Ph.D. degree in physics in the Walter Schottky Institute, Technical University of Munich, Garching, Germany.

His current research interests are electronic and optical properties of semiconductor nanostructures.

Tillmann Kubis was born in Ingolstadt, Germany, in 1978. He received the Diplom degree in physics from the Technical University of Munich, Garching, Germany, in 2004. He is currently working toward the Ph.D. degree in theoretical semiconductor physics in the Walter Schottky Institute, Technical University of Munich, Garching, Germany.

His research interests include the implementation of nonequilibrium Green's functions on realistic charge and spin transport in semiconductor nanostructures.

Matthias Sabathil was born in Hamburg, Germany, in 1974. He received the Diplom degree in physics from the University of Konstanz, Konstanz, Germany, and the Ph.D. degree in physics from the Technical University of Munich, Munich, Germany, in 2004.

He is currently with OSRAM Opto Semiconductors, Regensburg, Germany. His research interest is the modeling of InGaN LEDs.

Alex Trellakis was born in Rotterdam, Netherlands, in 1971. He received the Diplom degree in physics from the University of Bonn, Bonn, Germany, and the M.Sc. degree in computer science and the Ph.D. degree in physics from the University of Illinois, Urbana–Champaign.

Afterward, he joined the Science Applications International Corporation and Intel Corporation as an Engineer. He is currently an Assistant Professor with the Walter Schottky Institute, Technical University of Munich, Garching, Germany. His research interests are nanoscale semiconductor structures and devices and the numerical solution of partial differential equations.

Peter Vogl was born in Graz, Austria, in 1949. He received the Ph.D. degree in physics from the University of Graz, Graz, in 1974.

Since 1990, he has been a Professor with the Theoretical Semiconductor Physics Group, Walter Schottky Institute and the Department of Physics, Technical University of Munich, Garching, Germany. His current research interests include the electronic structure and charge carrier transport in semiconductors, ferroelectrics, magnetic materials, and conducting polymers.